Proteomic insights into the regulatory function of ARID1A in colon cancer cells

SIRIPAT ALUKSANASUWAN[1,2], KEERAKARN SOMSUAN[1,2], SASITHORN WANNA-UDOM[3], SITTIRUK ROYTRAKUL[4], ATTHAPAN MORCHANG[1,2], ARTITAYA RONGJUMNONG[1,2] and NATTHIYA SAKULSAK[3,5]

[1]School of Medicine, Mae Fah Luang University, Muang, Chiang Rai 57100, Thailand; [2]Cancer and Immunology Research Unit, Mae Fah Luang University, Muang, Chiang Rai 57100, Thailand; [3]Department of Anatomy, Faculty of Medical Science, Naresuan University, Muang, Phitsanulok 65000, Thailand; [4]Functional Proteomics Technology Laboratory, National Center for Genetic Engineering and Biotechnology, National Science and Technology Development Agency, Klongluang, Pathum Thani 12120, Thailand; [5]Faculty of Medicine, Praboromarajchanok Institute, Ministry of Public Health, Mueang, Nonthaburi 11000, Thailand

Abstract. The AT-rich interacting domain-containing protein 1A (ARID1A) is a tumor suppressor gene that has been implicated in several cancers, including colorectal cancer (CRC). The present study used a proteomic approach to elucidate the molecular mechanisms of ARID1A in CRC carcinogenesis. Stable ARID1A-overexpressing SW48 colon cancer cells were established using lentivirus transduction and the successful overexpression of ARID1A was confirmed by western blotting. Label-free quantitative proteomic analysis using liquid chromatography-tandem mass spectrometry identified 705 differentially altered proteins in the ARID1A-overexpressing cells, with 310 proteins significantly increased and 395 significantly decreased compared with empty vector control cells. Gene Ontology enrichment analysis highlighted the involvement of the altered proteins mainly in the Wnt signaling pathway. Western blotting supported these findings, as a decreased protein expression of Wnt target genes, including c-Myc, transcription factor T cell factor-1/7 and cyclin D1, were observed in ARID1A-overexpressing cells. Among the altered proteins involved in the Wnt signaling pathway, the interaction network analysis revealed that ARID1A exhibited a direct interaction with E3 ubiquitin-protein ligase zinc and ring finger 3 (ZNRF3), a negative regulator of the Wnt signaling pathway. Further analyses using the The Cancer Genome Atlas colon adenocarcinoma public dataset revealed that ZNRF3 expression significantly impacted the overall survival of patients with CRC and was positively correlated with ARID1A expression. Finally, an increased level of ZNRF3 in ARID1A-overexpressing cells was confirmed by western blotting. In conclusion, the findings of the present study suggest that ARID1A negatively regulates the Wnt signaling pathway through ZNRF3, which may contribute to CRC carcinogenesis.

Introduction

The AT-rich interacting domain-containing protein 1A (ARID1A) is a crucial subunit of the switch/sucrose non-fermentable (SWI/SNF) chromatin remodeling complex (1). It contains an AT-rich interaction domain (ARID) responsible for binding to DNA (2) and features multiple LXXLL motifs in the C-terminal region, known to facilitate interactions with nuclear hormone receptors (3). ARID1A helps direct SWI/SNF complexes to specific chromatin targets by interacting with other transcriptional regulatory factors and enhancing the affinity for binding to these sites, thereby altering chromatin accessibility for several nuclear factors (4). ARID1A serves essential roles in chromatin remodeling, chromosome organization, transcriptional and epigenetic regulation (5,6).

ARID1A is a tumor suppressor gene that has been reported to undergo mutations in several types of cancer (7-9). These mutations in ARID1A include missense or truncating mutations, as well as in-frame insertions or deletions (indels), which contribute to the loss of protein function (8,9). Previous studies have demonstrated the participation of ARID1A in several biological processes involved in carcinogenesis and tumor progression, such as cell cycle control, modulation of the immune response and regulation of several signaling pathways (10,11).

Correspondence to: Dr Siripat Aluksanasuwan, School of Medicine, Mae Fah Luang University, 365 Moo 12, Thasud, Muang, Chiang Rai 57100, Thailand
E-mail: siripat.alu@mfu.ac.th

Dr Natthiya Sakulsak, Faculty of Medicine, Praboromarajchanok Institute, Ministry of Public Health, Talad Kwan, Mueang, Nonthaburi 11000, Thailand
E-mail: natthiyas@pi.ac.th

ARID1A mutations are found in 3.6-66.7% of colorectal cancer (CRC) cases, and they are thought to be caused by mismatch defects (1,12). Previous studies have reported the prognostic and tumor suppressive roles of ARID1A in CRC. Immunohistochemical analyses have revealed a relatively high incidence of ARID1A protein loss (25.8%) in primary CRC tumors. Loss of ARID1A protein expression is associated with clinicopathological characteristics, including advanced tumor-node-metastasis stage, distant metastasis, poor pathological differentiation and worse overall survival in patients with CRC (13,14). Additionally, ARID1A expression is associated with immune cell infiltration and immunotherapeutic response in patients with CRC (15). ARID1A knockdown enhances the proliferation, migration, invasion and chemoresistance of CRC cells (16,17). Furthermore, ARID1A has been reported to promote the epithelial-mesenchymal transition (EMT) process by regulating the expression of vimentin and E-cadherin (18,19). However, the precise molecular mechanisms through which ARID1A regulates CRC carcinogenesis and progression are not yet fully understood.

Proteomics is a powerful tool that enables the comprehensive analysis of global protein changes in biological samples. It has been widely used in cancer research to unravel the molecular mechanisms of diseases and facilitate the discovery of biomarkers and therapeutic targets (20,21). In the present study, a comparative proteomic analysis of ARID1A-overexpressing colon cancer cells and empty vector control cells was performed. Subsequently, bioinformatics analysis was performed to gain novel insights into the molecular mechanisms through which ARID1A is involved in CRC carcinogenesis and progression. Moreover, the potential role of ARID1A in the regulation of the Wnt signaling pathway was assessed using western blotting.

Materials and methods

Establishment of ARID1A-overexpressing SW48 cells. The pLenti-puro (cat. no. 39481; Addgene, Inc.) and pLenti-puro-ARID1A (cat. no. 39478; Addgene, Inc.) were donated by Professor Ie-Ming Shih from John Hopkins University (22). The plasmid vectors were cloned into One Shot™ Stbl3™ Chemically Competent E.coli (cat. no. C737303; Invitrogen™; Thermo Fisher Scientific, Inc.) and extracted using the QIAprep Spin Miniprep Kit (Qiagen GmbH). Vector sizes were confirmed using 1% agarose gel electrophoresis and visualized using RedSafe™ (Intron Biotechnology, Inc.). SW48 and 293T cells were purchased from the American Type Culture Collection. Both cells were cultured in DMEM supplemented with 10% FBS and penicillin/streptomycin (100 mg/ml; Invitrogen™; Thermo Fisher Scientific, Inc.) at 37˚C with 5% CO_2 in a humidified chamber. Using a second-generation lentivirus system, 293T cell transfection was performed using Lipofectamine® 3000 (Invitrogen; Thermo Fisher Scientific, Inc.) for 16 h at 37˚C. For each transfection, 1.5 μg of either the pLenti-puro-ARID1A or pLenti-puro plasmid, 1 μg of packaging plasmid (psPAX2; cat. no. 12260; Addgene, Inc.), and 1 μg of envelope plasmid (pCMV-VSV-G; cat. no. 8454; Addgene, Inc.) (23) were used. The viral supernatants were harvested 48 h post-transfection, centrifuged at 2,000 x g for 5 min, and filtered through 0.45-μm pore size membrane filters.

Lentivirus at a multiplicity of infection value of 5 was used to transduce SW48 cells with an 8-mg/ml polybrene reagent (Sigma-Aldrich; Merck KGaA). After 24 h of transduction, the medium was replaced with a selection medium (culture medium supplemented with puromycin at a final concentration of 500 ng/ml; Invitrogen; Thermo Fisher Scientific, Inc.) to establish stable ARID1A-overexpressing cells. The stable cells were maintained in the selection medium (500 ng/ml puromycin).

Western blot analysis. The cells were lysed using RIPA buffer (Abcam) and protein concentration was determined using a Bradford assay (Bio-Rad Laboratories, Inc.). Equal amounts of protein from each sample (20 μg) were separated by 12% SDS-PAGE and transferred onto a nitrocellulose membrane. The membrane was incubated with 5% skimmed milk in PBS at 25˚C for 1 h. Subsequently, it was incubated with rabbit polyclonal anti-ARID1A (1:1,000; cat. no. HPA005456; Sigma-Aldrich; Merck KGaA), rabbit monoclonal anti-c-Myc (1:1,000; cat. no. 5605; Cell Signaling Technology, Inc.), rabbit monoclonal anti-T cell factor (TCF)1/7 (1:1,000; cat. no. 2203; Cell Signaling Technology, Inc.), rabbit monoclonal anti-cyclin D1 (1:1,000; cat. no. 2978; Cell Signaling Technology, Inc.), rabbit polyclonal anti-zinc and ring finger 3 (ZNRF3; 1:1,000; cat. no. DF14289; Affinity Biosciences), or mouse monoclonal anti-GAPDH (1:5,000; cat. no. ab8245; Abcam) antibodies at 4˚C overnight. Following three washes with PBS containing 0.05% Tween 20 (PBS-T), the membrane was further incubated with corresponding horseradish peroxidase-conjugated secondary anti-rabbit IgG (1:2,000; cat. no. 65-6120; dilution, Invitrogen; Thermo Fisher Scientific, Inc.) or anti-mouse IgG (1:5,000; cat. no. ab205719; Abcam) antibodies at 25˚C for 1 h. Following three additional washes with PBS-T, immunoreactive bands were visualized using Clarity™ Western ECL Substrate (Bio-Rad Laboratories, Inc.) and imaged using the ChemiDoc™ Touch Imaging System (Bio-Rad Laboratories, Inc.). The intensity of immunoreactive bands was assessed using Image Lab software (version 5.1; Bio-Rad Laboratories, Inc.). GAPDH was used as a loading control. The band intensity of the target protein was normalized to the corresponding loading control, and the relative value was subjected to statistical analysis.

Sample preparation for shotgun proteomics. The cells were placed in a 6-well plate at a density of 200,000 cells per well and cultured in a complete growth medium (DMEM supplemented with 10% FBS and 0.5 μg/ml puromycin) for 48 h at 37˚C. Following two washes with PBS, the cells were lysed with 0.5% SDS for effective extraction of both membrane-bound and cytoplasmic proteins. Subsequent precipitation with acetone was performed to remove contaminants and concentrate the proteins. The lysate was mixed with 2 volumes of cold acetone (-20˚C) and left to incubate at -20˚C for 12 h. Centrifugation at 10,000 x g for 15 min at 4˚C was used to collect protein precipitates. The resulting pellets were air-dried and stored at -20˚C until they were used for subsequent proteomic analysis. The protein concentration was determined using the Lowry assay with BSA as a standard protein (24). Protein samples (5 μg) were subjected to in-solution digestion. The samples were dissolved in 10 mM ammonium bicarbonate, disulfide

bonds were reduced using 5 mM dithiothreitol in 10 mM ammonium bicarbonate at 60˚C for 1 h, and sulfhydryl groups were alkylated using 15 mM iodoacetamide in 10 mM ammonium bicarbonate at room temperature for 45 min in the dark. Sequencing grade porcine trypsin (at a 1:20 ratio) was used to digest the protein sample for 16 h at 37˚C. The resulting tryptic peptides were dried using a speed vacuum concentrator and reconstituted in 0.1% formic acid for nano-liquid chromatography-tandem mass spectrometry (LC-MS/MS) analysis.

LC/MS-MS. The LC/MS-MS method was selected to achieve high sensitivity and resolution for peptide separation and identification. Label-free quantitative proteomic analysis was chosen due to its ability to provide a comprehensive and reproducible analysis of protein expression levels in complex biological samples without the need for expensive labeling reagents and intricate sample preparation (25,26). The tryptic peptide samples were prepared for injection into the UltiMate™ 3000 Nano/Capillary LC System (Thermo Fisher Scientific, Inc.) coupled to a ZenoTOF 7600 mass spectrometer (SCIEX). Briefly, 1 μl peptide digests underwent enrichment on a μ-Precolumn (300 μm i.d. x 5 mm) containing Acclaim™ PepMap™ 100 C18 HPLC column (5 μm; 100 A; Thermo Fisher Scientific, Inc.). Subsequently, separation occurred on a 75 μm I.D. x 15 cm Acclaim PepMap RSLC C18 column (2 μm, 100Å; nanoViper; Thermo Fisher Scientific, Inc.). The C18 column was maintained in a thermostatted column oven set to 60˚C. Solvents A and B containing 0.1% formic acid in water and 0.1% formic acid in 80% acetonitrile, respectively, were supplied to the analytical column. A gradient of 5-55% solvent B was used to elute the peptides at a constant flow rate of 0.30 μl/min over a period of 30 min. The ZenoTOF 7600 system consistently used specific source and gas settings throughout all acquisitions. These settings included maintaining ion source gas 1 at 8 psi, curtain gas at 35 psi, CAD gas at 7 psi, a source temperature of 200˚C, positive polarity and a spray voltage set to 3,300 V. The top 50 precursor ions with the highest abundance from the survey MS1 were chosen. MS2 spectra were collected in the 100-1,800 m/z range with a 50 msec accumulation time, used the Zeno trap. LC-MS analysis of each sample was performed in triplicate.

MS data analysis. Protein in individual samples was quantified using MaxQuant 2.2.0.0 (27), using the andromeda search engine to match MS/MS spectra with the UniProt *Homo sapiens* database (https://www.uniprot.org/proteomes/UP000005640) (27). Label-free quantitation was performed using standard settings, including parameters such as maximum of two miss cleavages, a mass tolerance of 0.6 daltons for main search, trypsin as the digesting enzyme, carbamidomethylation of cysteine as a fixed modification, and the oxidation of methionine and acetylation of the protein N-terminus as variable modifications. Protein identification required peptides with ≥7 amino acids and one unique peptide. Identified proteins with ≥2 peptides, including one unique peptide, were considered for further data analysis. Protein false discovery rate was maintained at 1%, determined using reversed search sequences. The maximal number of modifications per peptide was set to 5. The *Homo sapiens* proteome from UniProt served as the search FASTA file, whilst potential contaminants listed in the contaminants.fasta file provided by MaxQuant were automatically included to the search space. The resulting MaxQuantProteinGroups.txt file was imported into Perseus version 1.6.6.0 (28), and contaminants unrelated to any UPS1 protein were eliminated from the dataset. The three maximum intensities for each identified protein were used for statistical comparisons using an unpaired t-test with P<0.05 considered to indicate a statistically significant difference. The $\log_2$ ratios of the ARID1A-overexpressing sample and the control sample were calculated. Any intensity value of 0 was set to 0.001 to prevent division by 0. Differentially altered proteins between the ARID1A-overexpressing sample and the control sample were identified using a threshold of P<0.05 and a $\log_2$ ratio of ≥ 2 or ≤-2.

Bioinformatics analysis. The Database for Annotation, Visualization and Integrated Discovery (DAVID; https://david.ncifcrf.gov/summary.jsp) online tool (version v2023q4) (29,30) was used to perform Gene Ontology (GO) and Kyoto Encyclopedia of Genes and Genomes (KEGG) pathway enrichment analyses on differentially altered proteins. P<0.05 was considered to indicate a statistically significant enrichment. Bubble plot visualization of the enrichment results was performed using the GraphBio online tool (http://www.graphbio1.com/en/) (31). Interaction network analysis of altered proteins enriched in the Wnt signaling pathway was performed using GeneMANIA version 3.6.0 (https://genemania.org/) (32) with parameters set as follows: Organism 'Homo sapiens (human)' and network weighting 'Biological process based'. Survival analysis and expression correlation of ARID1A with ZNRF3 were analyzed using The Cancer Genome Atlas-colon adenocarcinoma (TCGA-COAD) dataset (33) using the Gene Expression Profiling Interactive Analysis 2 database (http://gepia2.cancer-pku.cn/) with default parameters (34).

Statistical analysis. GraphPad Prism version 8.0.1 (Dotmatics) was used for statistical analysis. An unpaired t-test was used to compare two datasets. P<0.05 was considered to indicate a statistically significant difference.

Results

Establishment of ARID1A-overexpressing SW48 cells. Following selection with puromycin, the level of ARID1A protein in the empty vector control and ARID1A-overexpressing cells was determined by western blotting. The results demonstrated that the ARID1A protein level was significantly higher in ARID1A-overexpressing cells compared with the empty vector control, confirming the successful overexpression of ARID1A in the cells (Fig. 1).

Proteomic analysis of altered proteins in ARID1A-overexpressing cells. Proteomic analysis was performed to identify a set of proteins differentially expressed following ARID1A overexpression. Protein samples derived from ARID1A-overexpressing and empty vector control cells were subjected to label-free quantitative analysis by LC-MS/MS. The proteomic analysis identified a total of 705 differentially altered proteins, including 310 significantly increased proteins (P<0.05; $\log_2$ ratio of ≥2) and 395
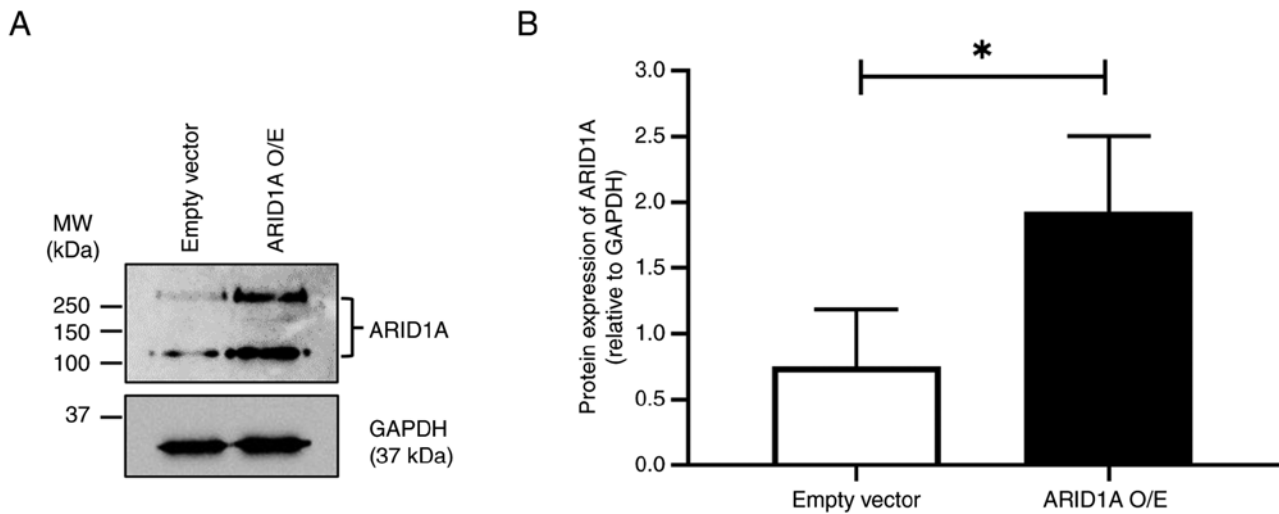
Figure 1. ARID1A protein expression in the empty vector control and ARID1A-overexpressing cells. (A) Western blot images of ARID1A and GAPDH (loading control). (B) Band intensity of ARID1A relative to GAPDH. The bar graph represents the mean ± standard deviation (n=3 per group). *P<0.05. ARID1A, AT-rich interacting domain-containing protein 1A; O/E, overexpression; MW, molecular weight.

significantly decreased proteins (P<0.05; log$_2$ ratio of ≤-2) in the ARID1A-overexpressing cells compared with the empty vector control cells. Detailed information on differentially altered proteins is presented in Table SI.

Functional enrichment analysis of differentially altered proteins. To assess the potential functions of ARID1A in colon cancer cells, GO and KEGG pathway enrichment analyses were performed on the differentially altered proteins. The results from DAVID revealed that differentially altered proteins in ARID1A-overexpressing cells were significantly enriched in several biological processes, including the 'Wnt signaling pathway', 'lipid metabolic process', and 'fat cell differentiation' (Fig. 2A). The majority of these altered proteins were located in the 'cytosol', 'cytoplasm' and 'nucleoplasm' (Fig. 2B). This analysis also identified several significantly enriched GO terms for molecular function, such as 'protein binding', 'metal ion binding' and 'carbohydrate binding' (Fig. 2C). KEGG pathway analysis indicated that these altered proteins were enriched in several pathways, including 'herpes simplex virus 1 infection', 'calcium signaling pathway', 'chemical carcinogenesis-receptor activation' and 'Wnt signaling pathway' (Fig. 2D). Detailed information on significantly enriched GO terms and KEGG pathways is summarized in Table SII.

Involvement of ARID1A and altered proteins in the Wnt signaling pathway. Functional enrichment analysis revealed the potential involvement of ARID1A in the Wnt signaling pathway (Fig. 3A). To assess this finding, the protein levels of Wnt-target genes, including c-Myc, TCF1/TCF7 and cyclin D1 were compared between the ARID1A-overexpressing cells and the empty vector control cells. The western blotting results demonstrated that ARID1A overexpression resulted in significant decreases of these Wnt-target genes compared with the empty vector control cells, suggesting a potential regulatory role of ARID1A in the Wnt signaling pathway (Fig. 3B and C).

Relationship between ARID1A and altered proteins in the Wnt signaling pathway. To gain a more comprehensive understanding of the roles of ARID1A in the aforementioned pathway, an interaction network was constructed using GeneMANIA to assess the relationships between ARID1A and the altered proteins involved in the Wnt signaling pathway. The results demonstrated that these proteins interact with each other mainly through 'Physical interactions' (77.64%), 'Co-expression' (8.01%) and 'Predicted' interactions (5.37%). Notably, ARID1A was demonstrated to directly interact with transcription factor 7 like 1 (TCF7L1) and ZNRF3 through 'Pathway' and 'Co-expression', respectively (Fig. 4A). Further analyses using the TCGA-COAD public dataset revealed that only ZNRF3, a negative regulator of the Wnt signaling pathway (35), had prognostic significance (Fig. 4B). Moreover, patients with COAD with a low ZNRF3 expression demonstrated significantly worse overall survival compared with those with a high expression (Fig. 4C). ZNRF3 expression was also significantly correlated with ARID1A expression in the database (Fig. 4D). These findings highlight the potential relationship between ARID1A and ZNRF3 in CRC carcinogenesis and progression.

Expression of ZNRF3 protein in ARID1A-overexpressing cells. Finally, the relationship between ARID1A and ZNRF3 was evaluated in the cells using western blotting. The results revealed that ARID1A-overexpressing cells had a significantly higher level of ZNRF3 protein expression compared with the empty vector control, suggesting a positive regulatory axis between these proteins (Fig. 5).

Discussion

ARID1A is an essential component of the SWI/SNF chromatin remodeling complex, which serves a crucial role in modulating the structure and accessibility of DNA (18). The diverse functions of ARID1A have been extensively documented in previous studies. These functions include chromatin
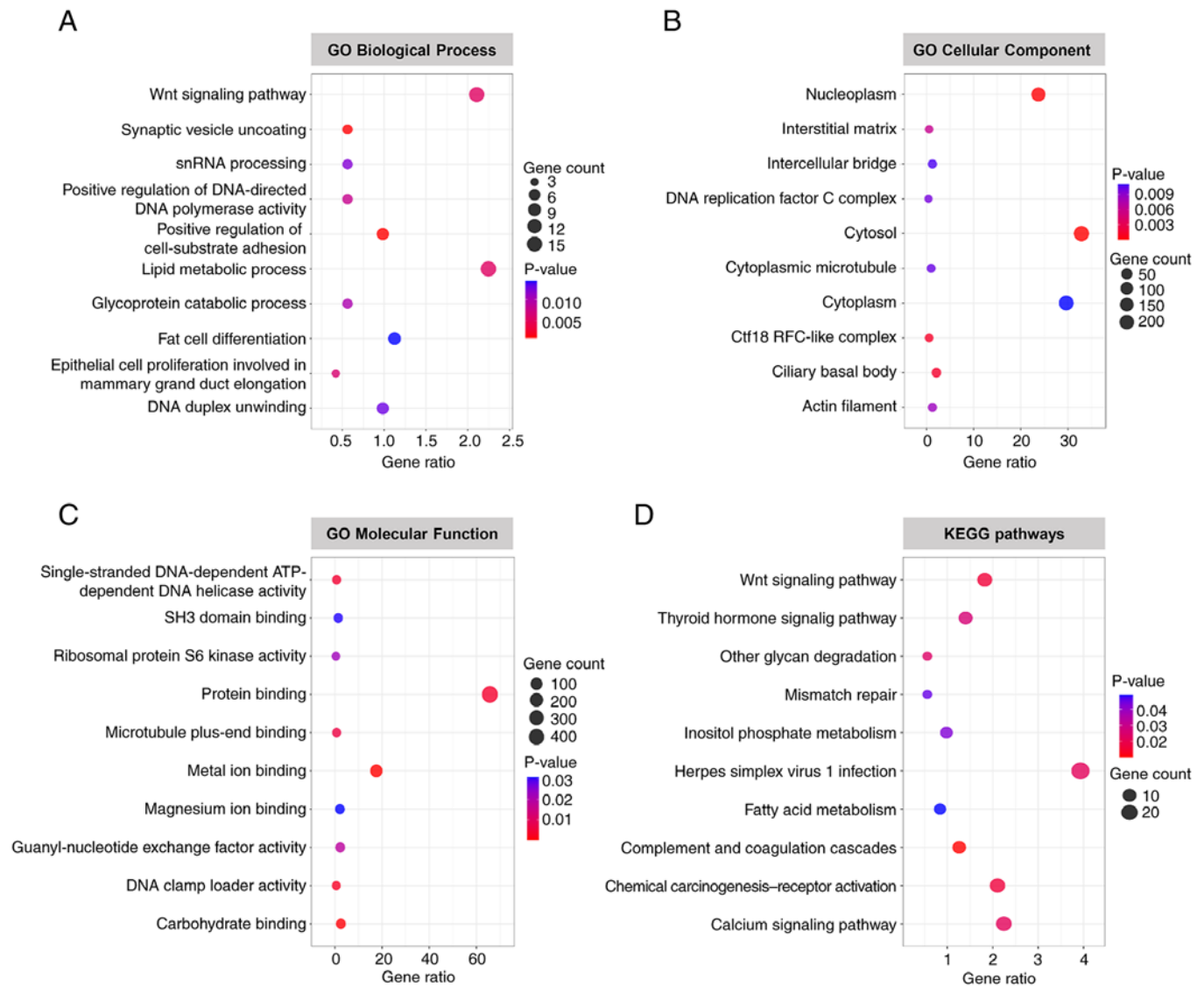
Figure 2. Functional enrichment analysis of differentially altered proteins. Bubble plot representing the top 10 significantly enriched GO (A) biological processes, (B) cellular components and (C) molecular functions, and (D) KEGG pathways. GO, Gene Ontology; KEGG, Kyoto Encyclopedia of Genes and Genomes; snRNA, small nuclear RNA; RFC, replication factor C; SH3, Src-homology 3.

remodeling, transcriptional regulation (5), oncogenic and tumor suppressor activity (36), microsatellite instability and immune checkpoint blockade (37), cell proliferation and differentiation (38), and epigenetic regulation (6). However, the specific functions of ARID1A can vary depending on the cell type and the cellular context (5,6,36-38). Thus, an understanding of its precise function in a specific cancer type is necessary.

In the present study, ARID1A-overexpressing SW48 cells were successfully established using lentivirus transduction. Furthermore, western blotting demonstrated two immunoreactive bands of ARID1A. ARID1A has a theoretical molecular weight of ~242 kDa (UniProt accession no. O14497), corresponding to the upper band detected at 250 kDa in the present study; however, several studies have reported multiple bands of ARID1A using western blotting (11,39,40). Therefore, it appears that the multiple bands detected represent ARID1A and possibly its degraded forms.

Previous studies have reported that ARID1A knockdown promotes carcinogenic behaviors (16-18), whilst its overexpression reverses such effects in CRC cells (19). These findings underscored the tumor suppressive role of ARID1A in CRC cells. Consequently, the present study primarily focused on elucidating its underlying mechanisms. Through proteomic analysis, 705 proteins that were differentially altered in ARID1A-overexpressing cells compared with empty vector control cells were identified. Functional enrichment analysis revealed a significant enrichment of these altered proteins in the Wnt signaling pathway, suggesting a potential functional association between ARID1A and this pathway.

Label-free quantitative proteomic analysis was chosen for the present study due to its cost-effectiveness and ability to provide comprehensive protein expression profiles without intricate sample preparation; however, it has limitations such as susceptibility to technical variability and lower sensitivity compared to labeled methods (25,26), potentially missing low-abundance proteins. To address these issues in future studies, rigorous sample preparation, use of internal standards, and validation with complementary techniques such as targeted
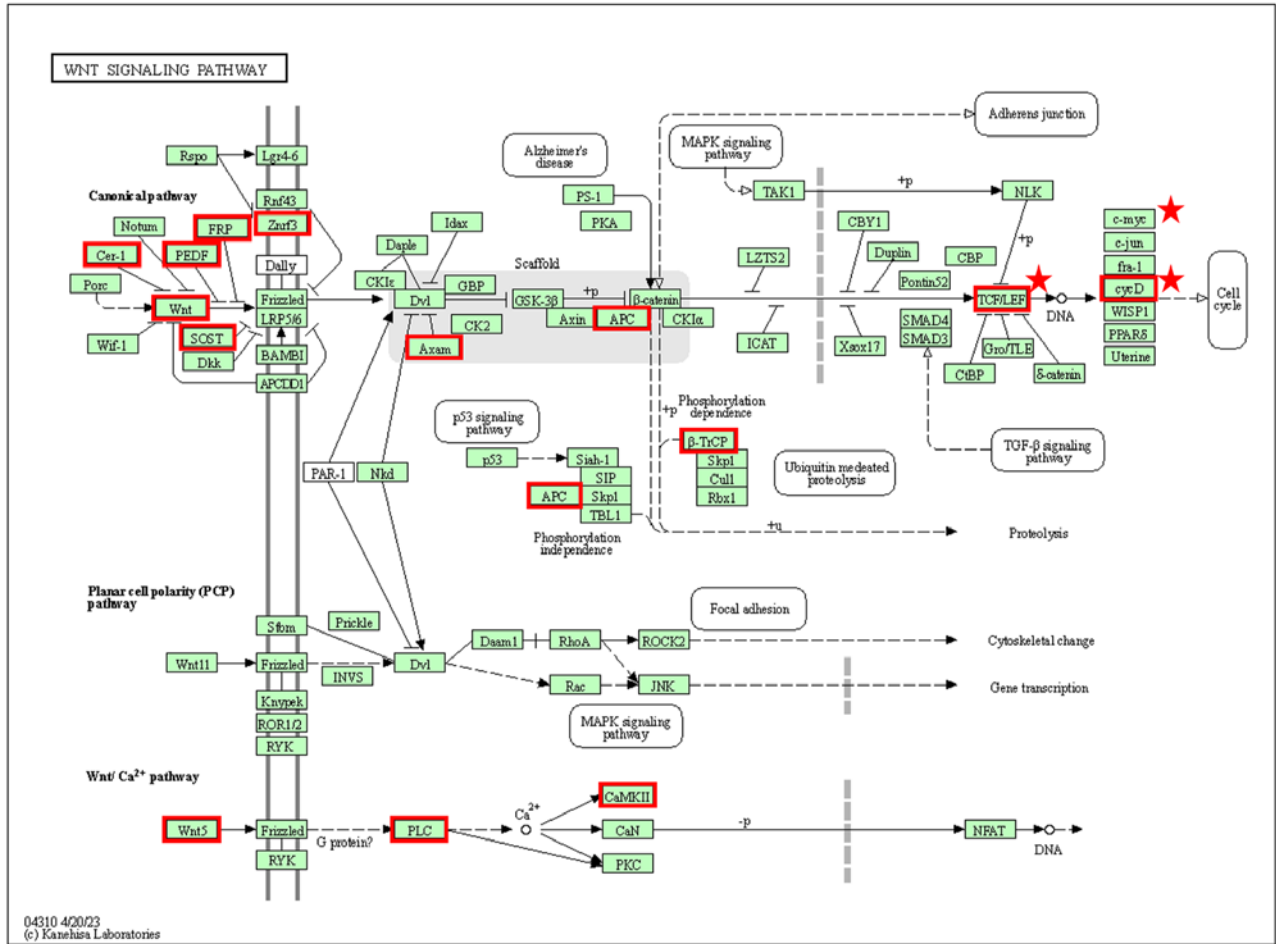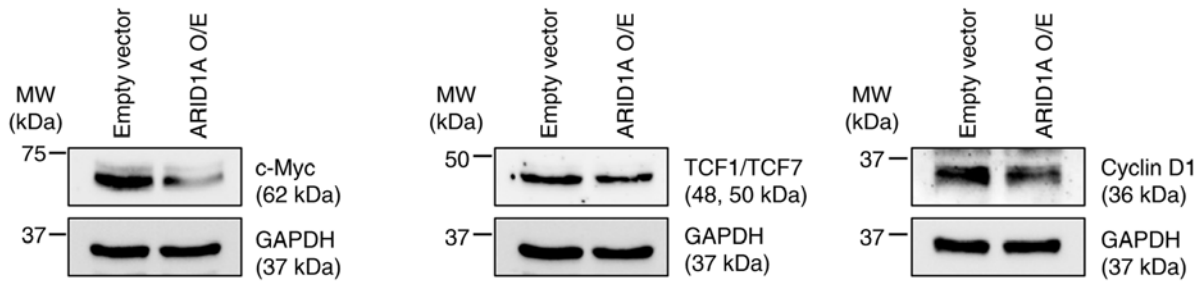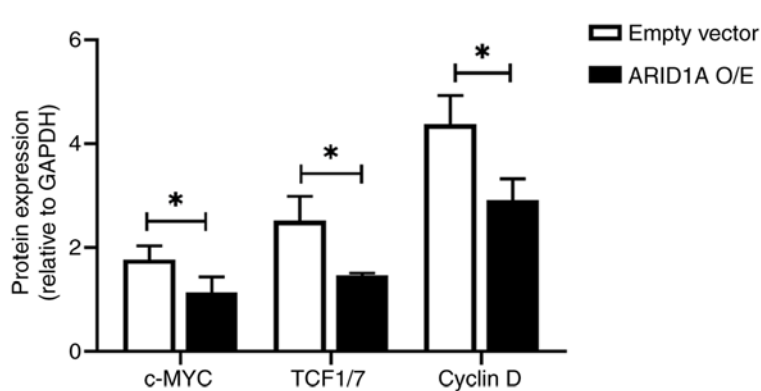
Figure 3. Involvement of ARID1A and altered proteins in the Wnt signaling pathway. (A) Wnt signaling pathway information generated using Kyoto Encyclopedia of Genes and Genomes (hsa04310). The pathway is illustrated using data from the KEGG database (https://www.genome.jp/pathway/hsa04310) (53). Red boxes indicate differentially altered proteins. (B) Western blot images for c-Myc, TCF1/TCF7 and cyclin D1, with GAPDH as the loading control. (C) Band intensity of proteins relative to GAPDH. The bar graph represents the mean ± standard deviation (n=3 per group). $^*P<0.05$. ARID1A, AT-rich interacting domain-containing protein 1A; TCF, T cell factor; O/E, overexpression; MW, molecular weight.
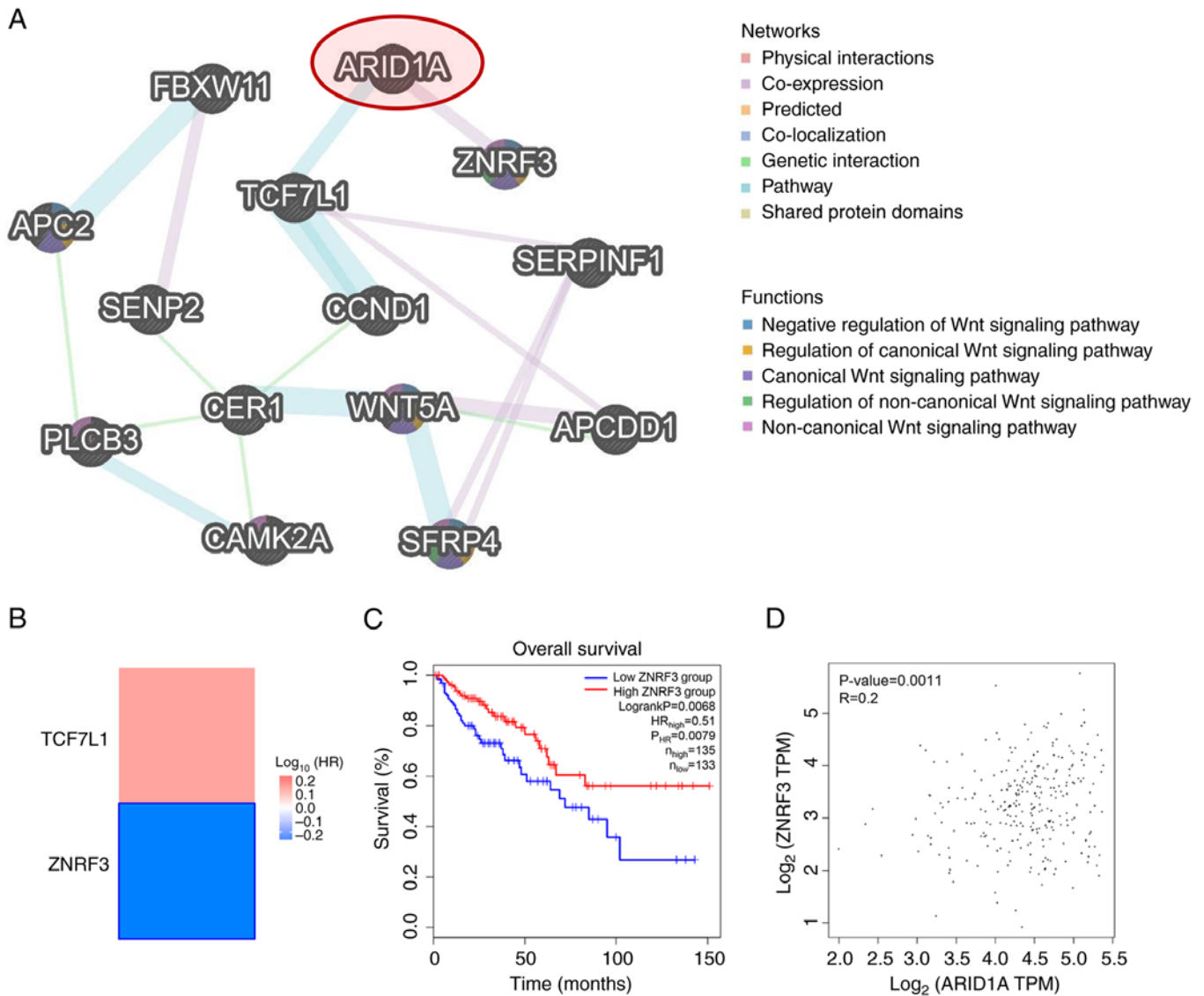
Figure 4. Association between ARID1A and altered proteins involved in the Wnt signaling pathway. (A) Interaction network of ARID1A and altered proteins involved in the Wnt signaling pathway constructed using GeneMANIA. (B) Heatmap of the HR of TCF7L1 and ZNRF3 for the overall survival of patients with COAD, created using GEPIA2. The framed block indicates a significant prognostic value. (C) Kaplan-Meier curve for overall survival of patients with COAD with different levels of ZNRF3 expression, plotted using GEPIA2. (D) Correlation between the expression of ARID1A and ZNRF3 in COAD, analyzed using GEPIA2. ARID1A, AT-rich interacting domain-containing protein 1A; TCF7L1, transcription factor 7 like 1; ZNRF3, zinc and ring finger 3; COAD, colon adenocarcinoma; GEPIA2, Gene Expression Profiling Interactive Analysis 2; HR, hazard ratio; TPM, transcripts per million.

proteomics or western blotting are recommended. Advances in instrumentation and software are expected to further enhance the reliability and accuracy of label-free proteomics (25,26).

The Wnt signaling pathway has been extensively studied and is known to serve a crucial role in several cellular processes associated with cancer, including cell proliferation, apoptosis and EMT (41). A previous study reported that the loss of ARID1A inhibited canonical WNT/β-catenin activity in human gastric cancer organoid lines (42). Downregulation of ARID1A and the Notch/Wnt signaling pathway-related genes have also been reported in gynecological tumors (43). In addition, ARID1A deletion in the intestines of mice in a previous study led to a decrease in the expression of target genes associated with the Wnt signaling pathway, such as achaete-scute family bHLH transcription factor 2, SRY-box transcription factor 9, axin 2, transcription factor 4, and hes

family bHLH transcription factor 1 (44). The data of the present study demonstrated that ARID1A overexpression resulted in a decreased expression of the Wnt-target genes in the cells. These findings suggest that ARID1A may exert its tumor suppressive activity by regulating the Wnt signaling pathway in CRC cells. However, the expression of WNT/β-catenin signaling components, such as β-catenin and its phosphorylated form, adenomatous polyposis coli, or serine/threonine kinase GSK-3 and its phosphorylated form, were not assessed in the present study. Clarifying the involvement of these key markers in future studies would be essential to validate the proposed relationship between ARID1A and the Wnt signaling pathway in CRC.

Through proteomic analysis, a significant increase of cyclin D1 in ARID1A-overexpressing cells was identified in the present study; however, its decreased level was detected
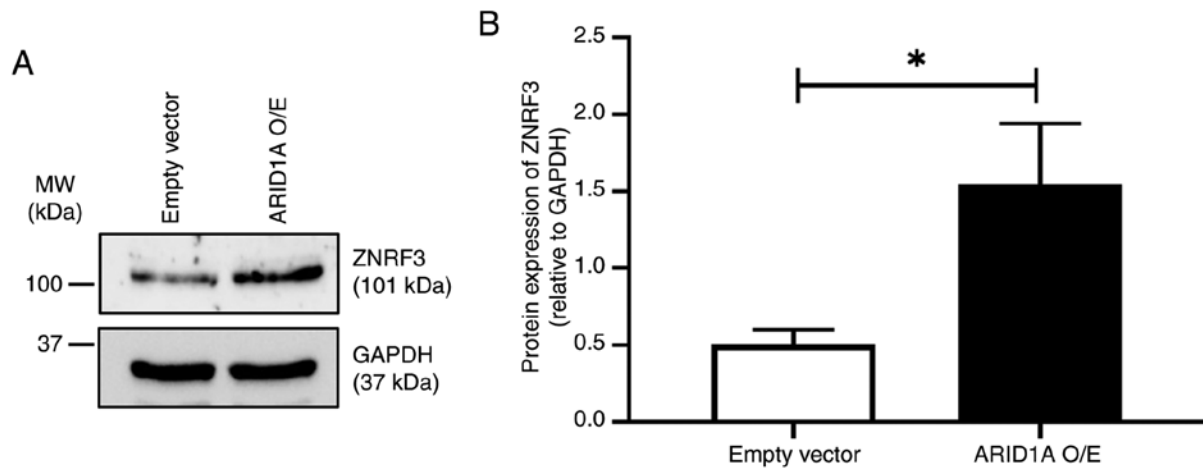
Figure 5. ZNRF3 protein expression in the empty vector control and ARID1A-overexpressing cells. (A) Western blot images of ZNRF3 and GAPDH (loading control) expression. (B) Band intensity of ZNRF3 expression relative to GAPDH. The bar graph represents the mean ± standard deviation (n=3 per group). *P<0.05. ZNRF3, zinc and ring finger 3; ARID1A, AT-rich interacting domain-containing protein 1A; O/E, overexpression; MW, molecular weight.

by western blotting. Whilst this specific discrepancy in cyclin D1 levels between LC-MS/MS and western blotting has not been reported before, such discrepancies between these techniques are common in proteomic studies (45-48). For instance, in a study by Pino *et al* (47), discrepancies between proteomic and western blot results were observed for several proteins, which the authors attributed to differences in sample preparation and detection techniques. Similarly, Zhang *et al* (48) reported discrepancies between 2D-difference gel electrophoresis and western blotting for acyl-coA thioesterase 2. The study attributed these differences to the low expression levels and issues with antibody specificity. LC-MS/MS and western blotting differ in sample preparation, detection methods and quantification approaches. LC-MS/MS quantifies protein levels using retention time, mass-to-charge ratio and ion intensities, whereas western blotting uses antibodies to detect specific proteins (25,26). The most likely explanation for this discrepancy is that cyclin D1 expression is influenced by post-translational modifications (PTMs) and isoforms. Cyclin D1 is a key regulator in cell cycle control and exists in two major isoforms (cyclin D1a and b) along with other truncating variants and PTMs (49,50). Aberrant expressions of cyclin D1 isoforms and variants are involved in the pathogenesis of cancer (49,50). Therefore, it is plausible that the observed increase in protein abundance by LC-MS/MS may include specific isoforms or PTMs that were not semi-quantified by western blotting. The observed discrepancy in the present study may indicate a potential alteration of cyclin D1 isoforms and PTMs induced by ARID1A overexpression.

Among the altered proteins associated with the Wnt signaling pathway, ARID1A was revealed to directly interact with TCF7L1 and ZNRF3 in the present study; however, only the expression of ZNRF3 had a significant prognostic impact on the overall survival of patients with COAD. ZNRF3 is a transmembrane E3 ubiquitin ligase that acts as a negative regulator of the Wnt signaling pathway (35). A previous study reported an association between ZNRF3 expression and survival outcomes in patients with CRC, with ZNRF3 overexpression promoting the apoptosis and inhibiting the proliferation of CRC cells (51). In the present study, proteomic analysis identified a significant increase in ZNRF3 levels in ARID1A-overexpressing cells. Interaction network analysis revealed a potential interaction with ARID1A through co-expression. The TCGA-COAD dataset demonstrated a positive correlation between ARID1A and ZNRF3 expression, further confirmed by western blotting. Hence, these findings suggest that the interaction between ARID1A with ZNRF3 may contribute to the carcinogenesis and progression of CRC. However, the present study did not confirm the physical interaction between these two proteins by co-immunoprecipitation or double immunofluorescence staining experiments. Further studies are needed to validate these interactions.

To the best of our knowledge, no previous study has reported a direct relationship between ARID1A and ZNRF3. A proposed mechanism for how ARID1A overexpression may result in increased ZNRF3 expression is through transcriptional regulation. ARID1A functions as a transcriptional regulator, modulating chromatin accessibility and transcription factor binding (4). It is possible that ARID1A could directly bind or interact with transcriptional co-factors or chromatin remodelers at the ZNRF3 promoter, leading to enhanced transcription and an increase in ZNRF3 mRNA levels. Alternatively, ARID1A may interact with other proteins that stabilize ZNRF3 mRNA or prevent its degradation, leading to increased ZNRF3 protein levels. Further experimental studies are needed to elucidate the precise molecular mechanisms underlying this interaction.

Whilst the present study provides insights into the role of ARID1A in colon cancer and its potential interactions with the Wnt signaling pathway, several limitations should be acknowledged. First, the study primarily focused on ARID1A overexpression and its effects on protein expression profiles in one colon cancer cell line (SW48). Further studies in CRC cells with different molecular characteristics are warranted to validate the present findings across a broader spectrum. Additionally, the lack of physiological assays, such as proliferation, migration, invasion, apoptosis and cell cycle progression, is a limitation. These assays are crucial to comprehensively understand the functional consequences

of ARID1A overexpression and its relationship with the Wnt signaling pathway in CRC carcinogenesis and metastasis. Experiments involving genetic manipulation or inhibitor treatment specific to Wnt signaling molecules are also necessary to obtain a deeper understanding. Furthermore, the observed discrepancy between proteomic and western blot analyses regarding cyclin D1 expression needs to be validated by different experimental approaches. Finally, further investigations are required to elucidate the underlying mechanisms of the regulatory axis between ARID1A and ZNRF3 in CRC.

In conclusion, a set of 705 differentially altered proteins were identified in ARID1A-overexpressing cells compared with control cells. These altered proteins were mainly involved in the Wnt signaling pathway. Bioinformatics analyses also highlighted a potential functional interaction between ARID1A and ZNRF3 in CRC carcinogenesis and progression. A better understanding of the role of ARID1A in CRC would help in the development of targeted therapies and diagnostic approaches for CRC.

Availability of data and materials

The raw mass-spectrometric data generated in the present study may be found in the ProteomeXchange Consortium via the jPOST repository (https://repository.jpostdb.org) (52) under accession numbers PXD052413 in the ProteomeXchange and JPST003117 in the jPOST repository, or at the following URLs: https://proteomecentral.proteomexchange.org/cgi/GetDataset?ID=PXD052413 and https://repository.jpostdb.org/entry/JPST003117, respectively. The other data generated in the current study may be requested from the corresponding author.

Authors' contributions

SA and KS contributed to the conception and design of the study, performed experiments, data analysis and visualization, and were major contributors to the writing of the manuscript. SW, AM and AR performed experiments and data analysis. SR performed the proteomic analysis. NS contributed to the conception and design of the study, data analysis, supervision, funding acquisition and manuscript editing. SA and NS confirm the authenticity of all the raw data. All authors read and approved the final manuscript.

Ethics approval and consent to participate

Not applicable.

Patient consent for publication

Not applicable.

Competing interests

The authors declare that they have no competing interests.

References

1. Zhao S, Wu W, Jiang Z, Tang F, Ding L, Xu W and Ruan L: Roles of ARID1A variations in colorectal cancer: A collaborative review. Mol Med 28: 42, 2022.
2. Wilsker D, Probst L, Wain HM, Maltais L, Tucker PW and Moran E: Nomenclature of the ARID family of DNA-binding proteins. Genomics 86: 242-251, 2005.
3. Wang X, Nagl NG, Wilsker D, Van Scoy M, Pacchione S, Yaciuk P, Dallas PB and Moran E: Two related ARID family proteins are alternative subunits of human SWI/SNF complexes. Biochem J 383: 319-325, 2004.
4. Wu RC, Wang TL and Shih IeM: The emerging roles of ARID1A in tumor suppression. Cancer Biol Ther 15: 655-664, 2014.
5. Liu X, Li Z, Wang Z, Liu F, Zhang L, Ke J, Xu X, Zhang Y, Yuan Y, Wei T, *et al*: Chromatin remodeling induced by ARID1A loss in lung cancer promotes glycolysis and confers JQ1 vulnerability. Cancer Res 82: 791-804, 2022.
6. Wilson MR, Reske JJ, Holladay J, Neupane S, Ngo J, Cuthrell N, Wegener M, Rhodes M, Adams M, Sheridan R, *et al*: ARID1A mutations promote P300-dependent endometrial invasion through super-enhancer hyperacetylation. Cell Rep 33: 108366, 2020.
7. Jiang T, Chen X, Su C, Ren S and Zhou C: Pan-cancer analysis of *ARID1A* alterations as biomarkers for immunotherapy outcomes. J Cancer 11: 776-780, 2020.
8. Fontana B, Gallerani G, Salamon I, Pace I, Roncarati R and Ferracin M: ARID1A in cancer: Friend or foe? Front Oncol 13: 1136248, 2023.
9. Guan B, Gao M, Wu CH, Wang TL and Shih IeM: Functional analysis of in-frame indel ARID1A mutations reveals new regulatory mechanisms of its tumor suppressor functions. Neoplasia 14: 986-993, 2012.
10. Mullen J, Kato S, Sicklick JK and Kurzrock R: Targeting ARID1A mutations in cancer. Cancer Treat Rev 100: 102287, 2021.
11. Somsuan K, Peerapen P, Boonmark W, Plumworasawat S, Samol R, Sakulsak N and Thongboonkerd V: *ARID1A* knockdown triggers epithelial-mesenchymal transition and carcinogenesis features of renal cells: Role in renal cell carcinoma. FASEB J 33: 12226-12239, 2019.
12. Xu S and Tang C: The role of *ARID1A* in tumors: Tumor initiation or tumor suppression? Front Oncol 11: 745187, 2021.
13. Wei XL, Wang DS, Xi SY, Wu WJ, Chen DL, Zeng ZL, Wang RY, Huang YX, Jin Y, Wang F, *et al*: Clinicopathologic and prognostic relevance of ARID1A protein loss in colorectal cancer. World J Gastroenterol 20: 18404-18412, 2014.
14. Ye J, Zhou Y, Weiser MR, Gönen M, Zhang L, Samdani T, Bacares R, DeLair D, Ivelja S, Vakiani E, *et al*: Immunohistochemical detection of ARID1A in colorectal carcinoma: Loss of staining is associated with sporadic microsatellite unstable tumors with medullary histology and high TNM stage. Hum Pathol 45: 2430-2436, 2014.
15. Guan X, Cui L, Ruan Y, Fang L, Dang T, Zhang Y and Liu C: Heterogeneous expression of ARID1A in colorectal cancer indicates distinguish immune landscape and efficacy of immunotherapy. Discov Oncol 15: 92, 2024.
16. Xie C, Fu L, Han Y, Li Q and Wang E: Decreased ARID1A expression facilitates cell proliferation and inhibits 5-fluorouracil-induced apoptosis in colorectal carcinoma. Tumour Biol 35: 7921-7927, 2014.
17. Peerapen P, Sueksakit K, Boonmark W, Yoodee S and Thongboonkerd V: ARID1A knockdown enhances carcinogenesis features and aggressiveness of Caco-2 colon cancer cells: An in vitro cellular mechanism study. J Cancer 13: 373-384, 2022.
18. Baldi S, Zhang Q, Zhang Z, Safi M, Khamgan H, Wu H, Zhang M, Qian Y, Gao Y, Shopit A, *et al*: ARID1A downregulation promotes cell proliferation and migration of colon cancer via VIM activation and CDH1 suppression. J Cell Mol Med 26: 5984-5997, 2022.

19. Erfani M, Zamani M, Hosseini SY, Mostafavi-Pour Z, Shafiee SM, Saeidnia M and Mokarram P: ARID1A regulates E-cadherin expression in colorectal cancer cells: A promising candidate therapeutic target. Mol Biol Rep 48: 6749-6756, 2021.

20. Kwon YW, Jo HS, Bae S, Seo Y, Song P, Song M and Yoon JH: Application of proteomics in cancer: Recent trends and approaches for biomarkers discovery. Front Med (Lausanne) 8: 747333, 2021.

21. Aluksanasuwan S, Somsuan K, Ngoenkam J, Chiangjong W, Rongjumnong A, Morchang A, Chutipongtanate S and Pongcharoen S: Knockdown of heat shock protein family D member 1 (HSPD1) in lung cancer cell altered secretome profile and cancer-associated fibroblast induction. Biochimica Biophys Acta Mol Cell Res 1871: 119736, 2024.

22. Guan B, Wang TL and Shih IeM: ARID1A, a factor that promotes formation of SWI/SNF-mediated chromatin remodeling, is a tumor suppressor in gynecologic cancers. Cancer Res 71: 6718-6727, 2011.

23. Stewart SA, Dykxhoorn DM, Palliser D, Mizuno H, Yu EY, An DS, Sabatini DM, Chen IS, Hahn WC, Sharp PA, *et al*: Lentivirus-delivered stable gene silencing by RNAi in primary cells. RNA 9: 493-501, 2003.

24. Lowry OH, Rosebrough NJ, Farr AL and Randall RJ: Protein measurement with the Folin phenol reagent. J Biol Chem 193: 265-275, 1951.

25. Zhu W, Smith JW and Huang CM: Mass spectrometry-based label-free quantitative proteomics. J Biomed Biotechnol 2010: 840518, 2010.

26. Neilson KA, Ali NA, Muralidharan S, Mirzaei M, Mariani M, Assadourian G, Lee A, van Sluyter SC and Haynes PA: Less label, more free: Approaches in label-free quantitative mass spectrometry. Proteomics 11: 535-553, 2011.

27. Tyanova S, Temu T and Cox J: The MaxQuant computational platform for mass spectrometry-based shotgun proteomics. Nat Protoc 11: 2301-2319, 2016.

28. Tyanova S, Temu T, Sinitcyn P, Carlson A, Hein MY, Geiger T, Mann M and Cox J: The perseus computational platform for comprehensive analysis of (prote)omics data. Nat Methods 13: 731-740, 2016.

29. Huang da W, Sherman BT and Lempicki RA: Systematic and integrative analysis of large gene lists using DAVID bioinformatics resources. Nat Protoc 4: 44-57, 2009.

30. Huang da W, Sherman BT and Lempicki RA: Bioinformatics enrichment tools: Paths toward the comprehensive functional analysis of large gene lists. Nucleic Acids Res 37: 1-13, 2009.

31. Zhao T and Wang Z: GraphBio: A shiny web app to easily perform popular visualization analysis for omics data. Front Genet 13: 957317, 2022.

32. Warde-Farley D, Donaldson SL, Comes O, Zuberi K, Badrawi R, Chao P, Franz M, Grouios C, Kazi F, Lopes CT, *et al*: The GeneMANIA prediction server: Biological network integration for gene prioritization and predicting gene function. Nucleic Acids Res(Web Server issue) 38: W214-W220, 2010.

33. Cancer Genome Atlas Research Network; Weinstein JN, Collisson EA, Mills GB, Shaw KR, Ozenberger BA, Ellrott K, Shmulevich I, Sander C and Stuart JM: The cancer genome atlas pan-cancer analysis project. Nat Genet 10: 1113-1120, 2013.

34. Tang Z, Kang B, Li C, Chen T and Zhang Z: GEPIA2: An enhanced web server for large-scale expression profiling and interactive analysis. Nucleic Acids Res 47: W556-W560, 2019.

35. Koo BK, Spit M, Jordens I, Low TY, Stange DE, van de Wetering M, van Es JH, Mohammed S, Heck AJ, Maurice MM and Clevers H: Tumour suppressor RNF43 is a stem-cell E3 ligase that induces endocytosis of Wnt receptors. Nature 488: 665-669, 2012.

36. Sun X, Wang SC, Wei Y, Luo X, Jia Y, Li L, Gopal P, Zhu M, Nassour I, Chuang JC, *et al*: Arid1a has context-dependent oncogenic and tumor suppressor functions in liver cancer. Cancer Cell 32: 574-589.e6, 2017.

37. Shen J, Ju Z, Zhao W, Wang L, Peng Y, Ge Z, Nagel ZD, Zou J, Wang C, Kapoor P, *et al*: ARID1A deficiency promotes mutability and potentiates therapeutic antitumor immunity unleashed by immune checkpoint blockade. Nat Med 24: 556-562, 2018.

38. Liu X, Dai SK, Liu PP and Liu CM: Arid1a regulates neural stem/progenitor cell proliferation and differentiation during cortical development. Cell Prolif 54: e13124, 2021.

39. Yoodee S, Peerapen P, Plumworasawat S and Thongboonkerd V: ARID1A knockdown in human endothelial cells directly induces angiogenesis by regulating angiopoietin-2 secretion and endothelial cell activity. Int J Biol Macromol 180: 1-13, 2021.

40. Yoodee S, Peerapen P, Plumworasawat S, Malaitad T and Thongboonkerd V: Identification and characterization of ARID1A-interacting proteins in renal tubular cells and their molecular regulation of angiogenesis. J Transl Med 21: 862, 2023.

41. Zhao H, Ming T, Tang S, Ren S, Yang H, Liu M, Tao Q and Xu H: Wnt signaling in colorectal cancer: Pathogenic role and therapeutic target. Mol Cancer 21: 144, 2022.

42. Lo YH, Kolahi KS, Du Y, Chang CY, Krokhotin A, Nair A, Sobba WD, Karlsson K, Jones SJ, Longacre TA, *et al*: A CRISPR/Cas9-engineered *ARID1A*-deficient human gastric cancer organoid model reveals essential and nonessential modes of oncogenic transformation. Cancer Discov 11: 1562-1581, 2021.

43. Vaicekauskaitė I, Dabkevičienė D, Šimienė J, Žilovič D, Čiurlienė R, Jarmalaitė S and Sabaliauskaitė R: *ARID1A*, NOTCH and WNT signature in gynaecological tumours. Int J Mol Sci 24: 5854, 2023.

44. Hiramatsu Y, Fukuda A, Ogawa S, Goto N, Ikuta K, Tsuda M, Matsumoto Y, Kimura Y, Yoshioka T, Takada Y, *et al*: Arid1a is essential for intestinal stem cells through Sox9 regulation. Proc Natl Acad Sci USA 116: 1704-1713, 2019.

45. Heunis T, Lamoliatte F, Marín-Rubio JL, Dannoura A and Trost M: Technical report: Targeted proteomic analysis reveals enrichment of atypical ubiquitin chains in contractile murine tissues. J Proteomics 229: 103963, 2020.

46. Hong X, Wang T, Du J, Hong Y, Yang CP, Xiao W, Li Y, Wang M, Sun H and Deng ZH: ITRAQ-based quantitative proteomic analysis reveals that VPS35 promotes the expression of MCM2-7 genes in HeLa cells. Sci Rep 12: 9700, 2022.

47. Pino JMV, Nishiduka ES, da Luz MHM, Silva VF, Antunes HKM, Tashima AK, Guedes PLR, de Souza AAL and Lee KS: Iron-deficient diet induces distinct protein profile related to energy metabolism in the striatum and hippocampus of adult rats. Nutr Neurosci 25: 207-218, 2022.

48. Zhang X, Morikawa K, Mori Y, Zong C, Zhang L, Garner E, Huang C, Wu W, Chang J, Nagashima D, *et al*: Proteomic analysis of liver proteins of mice exposed to 1,2-dichloropropane. Arch Toxicol 94: 2691-2705, 2020.

49. Van Dross R, Browning PJ and Pelling JC: Do truncated cyclins contribute to aberrant cyclin expression in cancer? Cell Cycle 5: 472-477, 2006.

50. Wang J, Su W, Zhang T, Zhang S, Lei H, Ma F, Shi M, Shi W, Xie X and Di C: Aberrant cyclin D1 splicing in cancer: From molecular mechanism to therapeutic modulation. Cell Death Dis 14: 244, 2023.

51. Yu N, Zhu H, Tao Y, Huang Y, Song X, Zhou Y, Li Y, Pei Q, Tan Q and Pei H: Association between prognostic survival of human colorectal carcinoma and ZNRF3 expression. Onco Targets Ther 9: 6679-6687, 2016.

52. Okuda S, Watanabe Y, Moriya Y, Kawano S, Yamamoto T, Matsumoto M, Takami T, Kobayashi D, Araki N, Yoshizawa AC, *et al*: jPOSTrepo: An international standard data repository for proteomes. Nucleic Acids Res 45: D1107-D1111, 2017.

53. Kanehisa M and Goto S: KEGG: Kyoto encyclopedia of genes and genomes. Nucleic Acids Res 28: 27-30, 2000.